



Chemical characteristics of rainwater in the tropical rainforest region in northwestern Borneo

Ninu Krishnan Modon Valappil¹ · Prasanna Mohan Viswanathan¹ · Vijith Hamza¹

Received: 11 November 2019 / Accepted: 1 June 2020 / Published online: 23 June 2020
© Springer-Verlag GmbH Germany, part of Springer Nature 2020

Abstract

A comprehensive study of the chemical composition of rainwater was carried out from October 2016 to September 2017 in the equatorial tropical rainforest region of northwestern Borneo. Monthly cumulative rainwater samples were collected from different locations in the Limbang River Basin (LRB) and were later categorized into seasonal samples representing northeast monsoon (NEM), southwest monsoon (SWM), and inter-monsoon (IM) periods. Physical parameters (pH, EC, TDS, DO, and turbidity), major ions (HCO_3^- , Cl^- , Ca^{2+} , Mg^{2+} , Na^+ , and K^+) and trace metals (Co, Ni, Cd, Fe, Mn, Pb, Zn, and Cu) were analyzed from collected rainwater samples. Rainwater is slightly alkaline with mean pH higher than 5.8. Chloride and bicarbonate are the most abundant ions, and the concentration of major ions in seasonal rainwater has shown slight variation which follows a descending order of $\text{HCO}_3^- > \text{Cl}^- > \text{Na}^+ > \text{Ca}^{2+} > \text{Mg}^{2+} > \text{K}^+$ in NEM and $\text{Cl}^- > \text{HCO}_3^- > \text{Na}^+ > \text{Ca}^{2+} > \text{K}^+ > \text{Mg}^{2+}$ in SWM and $\text{Cl}^- > \text{HCO}_3^- > \text{Na}^+ > \text{Ca}^{2+} > \text{Mg}^{2+} > \text{K}^+$ in IM period. Trace metals such as Fe and Ni have shown dominance in seasonal rainwater samples, and all the metals have shown variation in concentration in different seasons. Variation in chemical characteristic of seasonal rainwater samples identified through piper diagram indicates dominance of $\text{Ca}^{2+}\text{-Mg}^{2+}\text{-HCO}_3^-$ and mixed $\text{Ca}^{2+}\text{-Mg}^{2+}\text{-Cl}^-$ facies during NEM, SWM, and IM periods. Statistical analysis of the results through two-way ANOVA and Pearson's correlation also indicates significant variation in physico-chemical characteristics. This suggests a variation in contributing sources during the monsoon seasons. Factor analysis confirmed the source variation by explaining the total variance of 79.80%, 90.72%, and 90.52% with three factor components in NEM, SWM, and IM rainwater samples with different loading of parameters. Enrichment factor analysis revealed a combined contribution of marine and crustal sources except K^+ which was solely from crustal sources. Sample analysis of backward air mass trajectory supports all these findings by explaining seasonal variation in the source of pollutants reaching the study area. Overall, the results show that the chemical composition of seasonal rainwater samples in LRB was significantly influenced by natural as well as anthropogenic processes. These include (long-range and local) industrial activities, fossil fuel combustion, forest burning, transportation activities including road transport and shipping activities, and land-derived soil dust along with chemical constituents carried by seasonal wind.

Keywords Rainwater chemistry · Tropical region · Statistical analysis · Enrichment factors · Borneo

Introduction

Composition of rainwater is controlled by the atmospheric particulate and gaseous constituents originated locally or

transported from distant sources (Al-Khlaifat and Al-Khashman 2007; Zeri et al. 2016; Ojekunle et al. 2018). Higher-level industrial developments and forest fires in many countries amplified the pollution load in the atmosphere and thus by enriching specific chemical constituents in rainwater (Nriagu 1990; Brännvall et al. 1999; Cheng 2003; Wang et al. 2009; Kord and Kord 2011; Chambers et al. 2015; Francová et al. 2017; Rosca et al. 2019). Chemical characteristics of rainwater are the dominant environmental factor which controls the ecosystem health of the region (Niu et al. 2017; Akpan et al. 2018). Change from pure to polluted characteristics of rainwater might induce the environmental, ecosystem degradation and disturbance in biogeochemical cycle through

Responsible editor: Philippe Garrigues

✉ Ninu Krishnan Modon Valappil
mvninukrishna@gmail.com

¹ Department of Applied Geology, Faculty of Engineering and Science, Curtin University Malaysia, CDT 250, 98009 Miri, Sarawak, Malaysia

acid rain, eutrophication, and increased trace metal concentration (Lovett 1994; Hu et al. 2003; Mouli et al. 2005; Li et al. 2010; Ghimire et al. 2014; Graeff et al. 2018; Masood et al. 2019). However, many of the researchers have considered rainwater can wash off many pollutants in the atmosphere (Gordon et al. 2000; Topçu et al. 2002; Polkowska et al. 2005; Calvo et al. 2010; Niu et al. 2017; Graeff et al. 2018). Understanding of the chemical characteristics of rainwater is essential and time-demanding because of increased use and consumption of rainwater for domestic and drinking purposes (Moglia et al. 2015). This is tantamount to overcome the shortage of fresh water due to high level of pollution as well as non-availability caused by severe drought (Adugna et al. 2018). Besides this, anticipating the non-availability of fresh water for a long period, many local governments imposed the rainwater harvesting structure with residential and industrial buildings in many parts of the world (Postel 2000; Rogers and Hall 2003). In view of the requirement for establishing standards of rainwater chemistry and estimating its characteristics over a specific region and countries, numerous studies were carried out in different parts of the world (Báez et al. 2007; Sakihama et al. 2008; Al-Khashman 2009; Zhang et al. 2012; Cerqueira et al. 2014; Chon et al. 2015; Hasan et al. 2017; Xing et al. 2017; Uchiyama et al. 2019). Among this, analysis of spatial and temporal variation in chemical characteristics of rainwater to detect the effect of climate change over a region gained wide acceptance (Keller et al. 1991; Avila and Alarcón 1999; Lee et al. 2010; Kumar et al. 2014; Meera and Ahammed 2018; Suescún et al. 2019; Orué et al. 2019).

Rainwater chemistry will give information about the quality of the atmosphere by reflecting meteorological condition exists in the region (Cong et al. 2010; Baklanov et al. 2016; Rajeev et al. 2016; Rao et al. 2017; Ouyang et al. 2019). Research carried out at various locations in the world indicates the influence of natural as well as anthropogenic sources over the enrichment of chemical constituents present in rainwater (Durand et al. 1992; Zhang and Liu 2004; Al-Khashman 2009; Kumar et al. 2014; Hu and Cheng 2016; Steinnes and Lierhagen 2018; Szép et al. 2019). Along with this, location (nearness to coastal, urban, and industrial area), elevation and land use practices in the region also controls the overall chemistry of rainwater (Zhang et al. 2011; Rao et al. 2016). Considering Borneo as whole and east Malaysian regions specifically, very fewer attempts have been taken to assess the chemical characteristics of rainwater (Radojevic and Lim 1995; Zhong et al. 2001; Gomyo et al. 2008). Most studies reported from this region deals with the effect of forest burning, forest fire-generated haze, and dust over the chemical characteristics of rainwater, particularly on the acidity and heavy metal concentration (Crutzen and Andreae 1990; Radojevic and Tan 2000; Radojevic 2003; Nadzir et al. 2017). Understanding the gap in the research data related to the rainwater

chemistry of the region, as a first-time attempt, the present study was initiated. The objective of the present study was to characterize the rainwater chemistry during monsoon seasons in an equatorial tropical rainforest region of the Malaysian Borneo.

Study area

In order to understand the chemical characteristics of rainwater in the tropical rainforest region, in the present study, the Limbang River Basin (LRB) in the northern region of Sarawak state of Malaysia, Borneo situated between the N latitudes $03^{\circ} 47' 7''$ to $04^{\circ} 54'$ and E longitudes $114^{\circ} 46' 7''$ to $115^{\circ} 31' 30''$ was selected (Fig. 1). Limbang River originates from highly elevated mountain ranges (Batu Lawi and Gunung Murud) in the southern region of Sarawak. Limbang River flows a total length of 196 km before it joins the South China Sea through the Brunei Bay, and the basin covers a total area of 3950 km². LRB shows varying topographical features and relief varies in the range of 1 to above 2400 m. Rainfall in the river basin was dominated by monsoon characteristics, and LRB receives an annual average rainfall of 3851 mm. Monsoon seasons in the area span for a total of 10 months and was separated by short periods of inter-monsoon. Southwest monsoon (SWM) covers 5 months from May to September, and the northeast monsoon (NEM) covers another 5 months from November to March. These monsoon seasons are separated by individual inter-monsoon months of April and October. Considering the monsoon seasons, NEM receives more rainfall than SWM. Mean monthly rainfall is higher than 250 mm in most months and daily temperature fluctuation in the range of 16 to 34 °C with a mean of 26 °C. Though agricultural and plantation activities are present at local (paddy and fruit orchards) and at regional (oil palm plantations) scales, more than 90% of the river basin was covered by rainforests, i.e., primary, secondary, and montane forests. Geologically, the river basin is sedimentary in origin (shale, sandstone, silt, limestone, and recent coastal and riverine alluvium) (MGDM 2013). Furthermore, the region undergoes periodical haze and dust cover originated from forest burning and natural forest fire incident took place in Southeast Asian countries (Sabuti and Mohamed 2016).

Materials and methods

Sample collection

A total of 60 samples representing monthly cumulative rainwater for a period of 1 year (October 2016 to September 2017) were collected from spatially separated five locations in LRB (Fig. 1). Two polyethylene barrels (5 L), fitted with

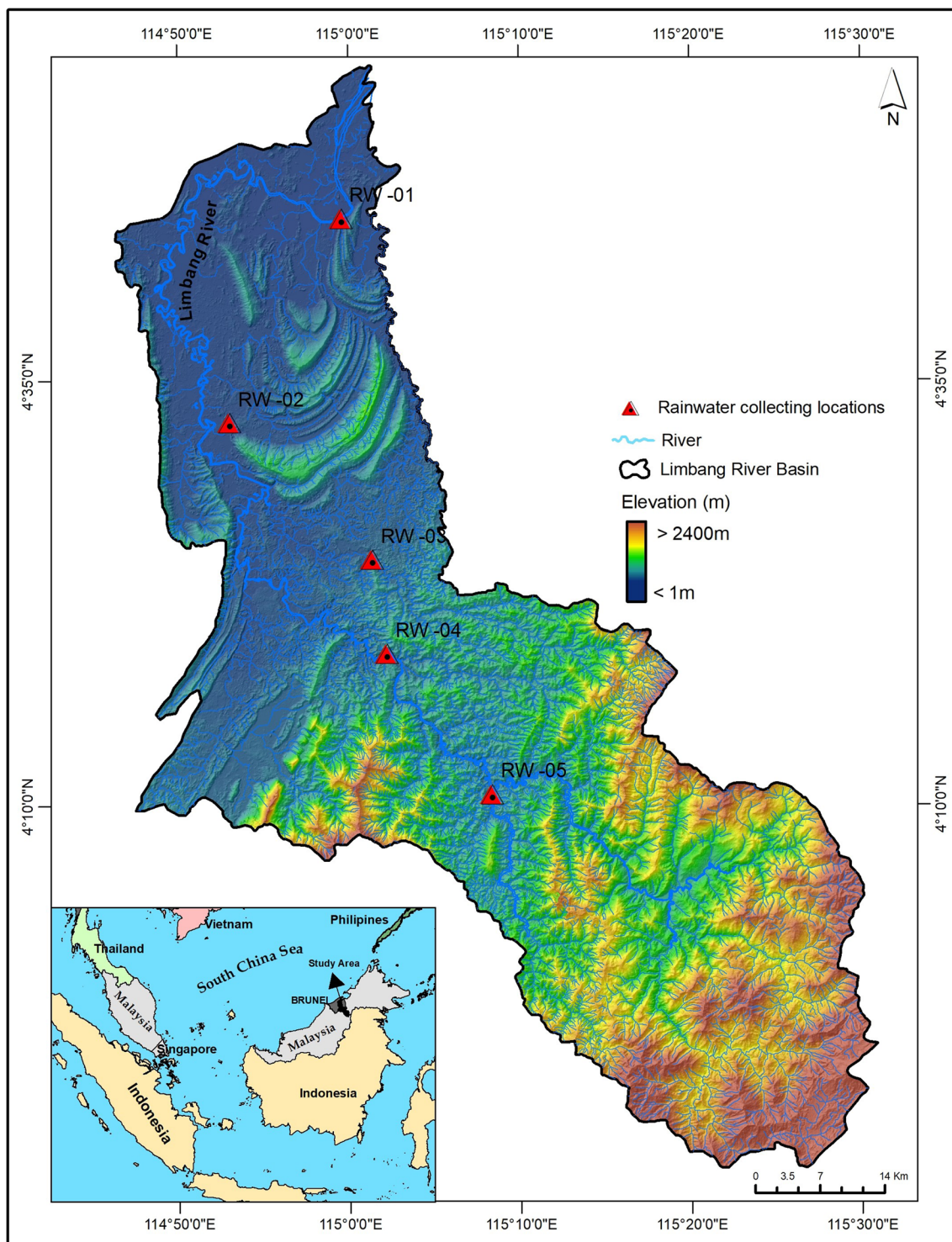


Fig. 1 Study area location map showing drainage networks and terrain elevation with rainwater sampling locations in the Limbang River basin (LRB)

funnels having 10-cm diameter, were used as the rainwater collector. In order to drain excess water, a small hosepipe was connected at the top end of the barrel. The whole rainwater collector unit was kept at an elevation to avoid other disturbances in sampling. Paraffin oil (0.5 cm thickness) was put in the container to avoid evaporation through the

walls. In order to avoid possible changes in the chemical characteristics of water, the whole sampling unit except rainwater collecting funnel was covered with heat-resistant material. Rainwater was collected from the first day of the month until the last day of the month. At the end of every month, the rainwater collected had to be shaken, but not

aggressively and was transferred to two 1-L polyethylene bottles after filtering using Whatman no.1 filter paper (11 μm) and was used for the analysis. Details of rainwater sampling locations are given in Table 1.

Analysis methods

Physico-chemical parameters such as pH, electrical conductivity (EC), total dissolved solids (TDS), dissolved oxygen (DO), and turbidity of rainwater were measured in the laboratory using portable pH, conductivity meter (Thermo Scientific Orion Star, 4 Star Plus Meter), and Hach meter (Hach® DR2800 spectrophotometer). Bicarbonate (HCO₃⁻) and chloride (Cl⁻) were determined by titrimetric method (APHA 1995, 2012). Later, the water samples were filtered using 0.45 μm Millipore filter paper and digested using 10 mL con. nitric acid (HNO₃) to lower the pH ~ 2 and make to 10 mL by heating around 60–70 °C using a hotplate. The concentrated sample is then remade to 100 mL using ultra-pure water for the analysis of trace metals (Cu, Pb, Fe, Mn, Zn, Cd, Ni, Co, Ca²⁺, Mg²⁺, Na⁺, and K⁺) using Atomic Absorption Spectrophotometer (Perkin Elmer Analyst 400).

Furthermore, the analysis results are separated into three different seasons such as northeast monsoon (NEM), southwest monsoon (SWM), and inter-monsoon (IM) and then interpreted, and the mean values were compared with other studies carried out in different parts of the world. Statistical analysis such as Pearson’s correlation, ANOVA, and factor analysis was also applied to detect the inter-relationships, variation, and source contribution of ions in seasonal rainfall over LRB. Furthermore, in order to identify the source contribution of chemical constituents in different seasons, a sample air mass back trajectory analysis was also conducted for individual seasons using a HYbrid Single-Particle Lagrangian Integrated Trajectory (HYSPLIT) transport model provided by the US National Atmospheric and Oceanic Administration (NOAA) Air Resources Laboratory (ARL).

Table 2 Details of meteorological parameters measured during the study period

Month	Mean rainfall (mm)	Rainy days	Mean temperature (°C)
Oct. 16	275	21	25.6
Nov. 16	396	25	25.3
Dec. 16	315	21	25.6
Jan. 17	314	19	25.2
Feb. 17	343	18	25.2
Mar. 17	428	26	25.7
Apr. 17	363	22	26.1
May. 17	572	26	26.1
Jun. 17	343	19	25.9
Jul. 17	179	15	25.8
Aug. 17	524	21	25.9
Sep. 17	350	22	25.8

Results and discussion

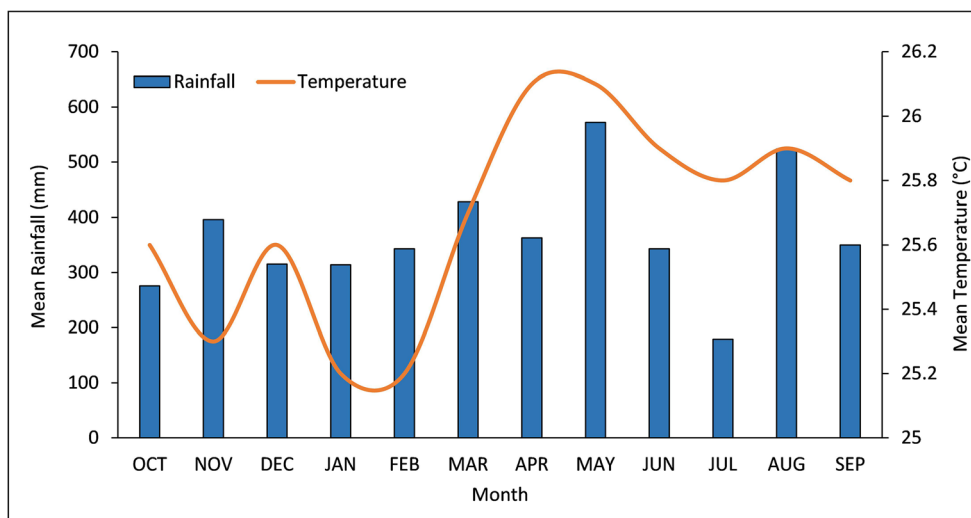
Meteorological characteristics

Basic meteorological characteristics of LRB during the period of study (October 2016 to September 2017) are given in Table 2 and the mean temperature and rainfall during the sampling periods are shown in Fig. 2. Rainwater sampling was started in the month of October, which marks the inter-monsoon period. Following the inter-monsoon period, northeast monsoon (NEM) started in November and continued up to March (5 months). Then the second inter-monsoon month April followed by the southwest monsoon (SWM) continued for another 5 months from May to September. Mean monthly rainfall during the sampling period varies in the range of 179 (July 2017) to 572 mm (May 2017). Considering the seasonal rainfall characteristics, during NEM, mean rainfall varies from 314 (January 2017) to 428 mm (March 2017), whereas in SWM, rainfall ranges from 179 (July 2017) to 572 mm (May 2017). IM

Table 1 Details of rainwater collection locations in the Limbang River Basin

Sampling locations	Latitude	Longitude	Elevation (m)	Area characteristics
RW-01	4.741306	114.9946	3	Urban area, located near to Limbang River
RW-02	4.541222	114.8853	28	Rural area, located away from Limbang river, agricultural land, and tropical forest present
RW-03	4.406889	115.0244	52	Undeveloped area, inside tropical forest, higher level of human activity in relation to logging. Near to tributary of Limbang River
RW-04	4.314722	115.0383	131	Undeveloped area, inside tropical forest, settlements are present, near to Limbang River
RW-05	4.176778	115.1408	161	Undeveloped area, inside tropical forest, settlements, and agricultural activities are present. Near to tributary of Limbang River

Fig. 2 Temporal distribution of mean monthly rainfall and temperature in LRB during the period of study



period October received a mean rainfall of 275 mm and April recorded 363 mm. Mean rainy days in LRB during the sampling periods vary between 15 (July 2017) and 26 days (March, May 2017). Mean temperature during the study period ranges from 25.2 (January and February 2017) to 26.1 °C (April and March 2017). It was noted that, during the study period, LRB recorded comparatively higher amount of monthly rainfall in most months, and mean monthly rainfall was above 360 mm against the annual rainfall of 4402 mm.

Physical characteristics of rainwater

Results of parameters such as pH, EC, TDS, DO, and turbidity of the rainwater collected during different seasons (NEM, SWM, and IM) were provided in Table 3, and its temporal variation is shown in Fig. 3. During NEM, pH varies in the range of 5.25 to 7.14 with a mean of 5.86. EC varies from 47.95 to 88.20 μS/cm with a mean of 69.11 μS/cm. TDS shows variation from 33.57 to 61.74 mg/L with a mean of 48.37 mg/L. DO during the period ranges from 6.30 to 9.19

Table 3 Results of physico-chemical parameters analyzed from seasonal rainwater collected from LRB

Parameters	NEM			SWM			IM		
	Min	Max	Mean	Min	Max	Mean	Min	Max	Mean
pH	5.25	7.14	5.86	5.53	7.23	6.14	5.59	7.22	6.08
EC (μS/cm)	47.95	88.2	69.11	95.16	260.77	116.98	44.94	119.46	79.89
TDS (mg/L)	33.57	61.74	48.37	66.61	182.54	81.88	31.46	83.62	55.93
DO (mg/L)	6.30	9.19	7.66	3.70	7.60	6.24	3.40	8.71	6.45
Turbidity (NTU)	0.04	3.30	0.97	0.04	4.92	1.06	0.03	1.08	0.40
Bicarbonate (mg/L)	12.2	43.19	30.07	30.50	59.48	36.60	9.15	35.08	25.35
Chloride (mg/L)	12.78	18.46	16.43	31.91	69.13	39.60	13.29	48.74	28.04
Ca (mg/L)	0.281	1.254	0.62	0.361	17.16	1.38	0.515	1.323	0.85
Mg (mg/L)	0.182	1.98	0.38	0.129	3.49	0.34	0.19	0.77	0.41
Na (mg/L)	0.294	2.47	0.73	0.215	46.44	3.34	0.268	2.30	1.07
K (mg/L)	0.035	0.375	0.15	0.068	6.68	0.62	0.105	0.531	0.20
Co (mg/L)	0.013	0.056	0.03	0.005	0.032	0.02	0.011	0.045	0.03
Ni (mg/L)	0.087	0.219	0.18	0.063	0.161	0.10	0.082	0.19	0.12
Cd (mg/L)	0.003	0.008	0.005	0.002	0.011	0.005	0.003	0.009	0.006
Fe (mg/L)	0.681	1.643	1.07	0.625	1.158	0.95	0.775	1.705	1.26
Mn (mg/L)	0.016	0.043	0.03	0.016	0.045	0.03	0.018	0.038	0.03
Pb (mg/L)	0.007	0.115	0.04	0.012	0.035	0.02	0.018	0.109	0.05
Zn (mg/L)	0.013	0.033	0.02	0.001	0.025	0.01	0.001	0.031	0.02
Cu (mg/L)	0.008	0.026	0.02	0.006	0.016	0.01	0.003	0.019	0.01

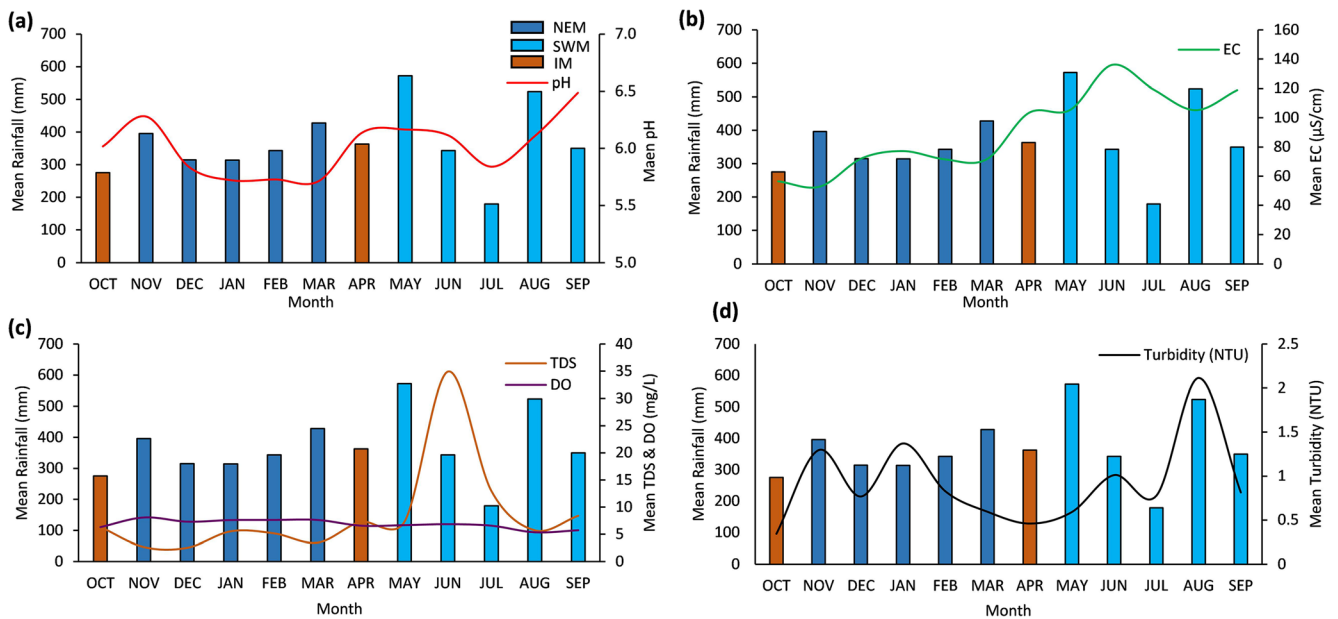


Fig. 3 Showing the temporal (season-wise) distribution of selected mean pH, EC, TDS, DO, and turbidity during the study period

9.19 mg/L and shows a mean of 7.66 mg/L. Turbidity varies in the range of 0.04 to 3.30NTU with a mean of 0.97NTU. In the case of SWM season, pH varies in the range of 5.53 to 7.23 with a mean of 6.14. EC varies from 95.16 to 260.77 µS/cm with a mean of 116.98 µS/cm. TDS varies in the range of 66.61 to 182.54 mg/L with a mean of 81.88 mg/L. DO during the period ranges from 3.70 to 7.60 mg/L and shows a mean of 6.24 mg/L. Turbidity varies in the range of 0.04 to 4.92 NTU with a mean of 1.06 NTU. At the same time, during the IM season, pH varies in the range of 5.59 to 7.22 with a mean of 6.08. EC varies from 44.94 to 119.46 µS/cm with a mean of 79.89 µS/cm. TDS shows variation in the range of 31.46 to 83.62 mg/L with a mean of 55.93 mg/L. DO during the period ranges from 3.40 to 8.71 mg/L and shows a mean of 6.45 mg/L. Turbidity varies in the range of 0.03 to 1.08 NTU with a mean of 0.40 NTU.

Physico-chemical characteristics of rainwater collected during different seasons from LRB show slight variation in its concentration. Mean concentration of pH in LRB is found to be varied, and the lowest mean pH was observed during NEM, whereas the SWM shows the highest. It was suggested that, rainwater falling through clean atmosphere shows pH value 5.6 which can be attributed to the dissolution of CO₂ present in the rain droplets (Bouhel et al. 1994; Al-Khashman 2009). The rainwater samples collected show slightly higher mean pH, and this might be due to the local influence of evaporation over rainfall characteristics in the specific seasons and also due to the presence of increased amount of particulate matter in the atmosphere (Galloway et al. 1982; Sanhueza et al. 1989; Rajeev et al. 2016). At the same time, considering the electrical conductivity (EC) and total dissolved solids (TDS), the lowest value of mean EC and TDS was noted during NEM, whereas the highest value was recorded in

SWM. The variability in the value range can be attributed to the local influence, and EC and TDS measured at different seasons indicates the relatively varying nature of dissolved ions concentration in rainwater (Abulude et al. 2018). This is because EC is directly proportional to TDS, which heavily depends on the concentration of dissolved ions, ionic strength, and temperature of water (Marandi et al. 2013). However, considering the mean concentration of DO in the rainwater collected in all seasons shows higher amount and was controlled by the structure of the raincloud and is also linked to the mechanism of raindrop formation and height of cloud base (Komabayasi 1959). Similarly the measured turbidity of rainwater in all the seasonal samples shows lower values suggesting the least presence of suspended particulate matter present in the atmosphere (Cobbina et al. 2013).

Chemical composition of rainwater

In addition to the physical parameters, major ions and trace metals in the rainwater collected during different seasons (NEM, SWM, and IM) were also analyzed in the present study (Table 3). During NEM, anions HCO₃⁻ and Cl⁻ vary in the range of 12.20 to 43.19 mg/L and 12.78 to 18.46 mg/L with a mean of 30.07 mg/L and 16.43 mg/L respectively. Cations analyzed during the season varies in the range of 0.281 to 1.254 mg/L with a mean of 0.62 mg/L (Ca²⁺), 0.182 to 1.98 mg/L with a mean of 0.38 mg/L (Mg²⁺), 0.294 to 2.47 mg/L with a mean of 0.73 mg/L (Na⁺), and 0.035 to 0.375 mg/L with mean of 0.15 mg/L (K⁺). In SWM, HCO₃⁻ and Cl⁻ vary in the range of 30.50 to 59.48 mg/L and 31.91 to 69.13 mg/L with a mean of 36.60 mg/L and 39.60 mg/L respectively. Cations analyzed during the season vary in the range of 0.361 to 17.16 mg/L with a mean of 1.38 mg/L

(Ca²⁺), 0.129 to 3.49 mg/L with a mean of 0.34 mg/L (Mg²⁺), 0.215 to 46.44 mg/L with a mean of 3.34 mg/L (Na⁺), and 0.068 to 6.68 mg/L with mean of 0.62 mg/L (K⁺). At the same time, during IM periods, HCO₃⁻ and Cl⁻ vary in the range of 9.15 to 35.08 mg/L and 13.29 to 48.74 mg/L with a mean of 25.35 mg/L and 28.04 mg/L respectively. Cations analyzed during the season vary in the range of 0.515 to 1.323 mg/L with a mean of 0.85 mg/L (Ca²⁺), 0.19 to 0.77 mg/L with a mean of 0.41 mg/L (Mg²⁺), 0.268 to 2.30 mg/L with a mean of 1.07 mg/L (Na⁺), and 0.105 to 0.531 mg/L with mean of 0.20 mg/L (K⁺). Furthermore, it was noted that though the concentration of major ions in rainwater in different seasons showed slight variation, ions in rainwater of NEM follow a general pattern of decreasing order of HCO₃⁻ > Cl⁻ > Na⁺ > Ca²⁺ > Mg²⁺ > K⁺; in SWM, the order was Cl⁻ > HCO₃⁻ > Na⁺ > Ca²⁺ > K⁺ > Mg²⁺; and in IM periods, the major ions follow the decreasing order of Cl⁻ > HCO₃⁻ > Na⁺ > Ca²⁺ > Mg²⁺ > K⁺.

Considering the concentration of major ions in rainwater samples corresponding to the seasons, it was noted that Cl⁻, HCO₃⁻, Na⁺, and Ca²⁺ dominate in all the seasons with varying concentrations of K⁺ and Mg²⁺. Higher concentration of HCO₃⁻ is due to the increased amount of CO₂ in the atmosphere, which reacts with water vapor to form HCO₃⁻, and the major driving force behind the mechanism might be the biomass burning in Southeast Asian countries (Hu et al. 2003; Khoon et al. 2011). Higher concentration of Cl⁻ in rainwater can be attributed by the marine contribution (evaporation of water from the South China Sea) and local evaporation from a land region which contains soil and rocks of calcareous origin (Al Obaidy and Joshi 2006; Khoon et al. 2011). In LRB, most of the areas are covered with calcareous soils, and the concentration of Ca²⁺ observed in the rainwater samples collected from these regions can be attributed to the dominance of dust particles which evolved from calcareous soils along with rapid evaporation at a local scale and re-precipitation which is typical in Borneo (Matawle et al. 2015; Rao et al. 2016). Dispersion of soil and biological fragments and excess emission of alkaline dust are the major sources of dissolved Mg²⁺ and Ca²⁺ in rainwater (Tsukuda et al. 2006; Sapek 2014). As discussed previously, calcareous soil in the region along with local and site-specific evaporation, which contributes to the precipitation in the region, controls the Ca²⁺ and Mg²⁺ concentration of the rainwater in the region. Concentration of Na⁺ and K⁺ in rainwater is mainly of marine contribution and are due to the presence of aerosols and evaporation-based sea salt in the atmosphere (Cerqueira et al. 2014). The study area is very close to the South China Sea, and most of the time, the cloud movement in the region was controlled by wind blowing from the South China Sea. Marine evaporation along with soil dust particles that evolved from the land surface might also contribute to the occurrence of Na⁺ and K⁺ in rainwater samples collected from LRB.

Trace metal concentration

Minimum, maximum, and mean values of trace metal in seasonal rainfall in LRB have shown variation between seasons, and the results are shown in Table 3. During NEM, Co, Ni, Cd, Fe, Mn, Pb, Zn, and Cu showed a mean concentration of 0.03, 0.18, 0.005, 1.07, 0.03, 0.04, 0.02, and 0.02 mg/L respectively. In SWM, trace metal has shown a slight decrease in concentration and are 0.02, 0.10, 0.005, 0.95, 0.03, 0.02, 0.01, and 0.01 mg/L for Co, Ni, Cd, Fe, Mn, Pb, Zn, and Cu respectively. Considering the IM periods, rainwater shows variation in the concentration of certain metals compared with NEM and SWM seasons. Trace metal concentration during the season was 0.03, 0.12, 0.006, 1.26, 0.03, 0.05, 0.02, and 0.01 mg/L for Co, Ni, Cd, Fe, Mn, Pb, Zn, and Cu respectively. Relative abundance of trace metals in rainwater samples collected during NEM follows the decreasing order of Fe > Ni > Pb > Mn > Co > Cu > Zn > Cd; during SWM, the order was Fe > Ni > Mn > Pb > Co > Cu > Zn > Cd; and for the IM season, the concentration of trace metals follows the decreasing order of Fe > Ni > Pb > Mn > Co > Zn > Cu > Cd respectively.

In general, trace metal concentration in rainwater was contributed by different natural as well as anthropogenic processes occurring in the region (Jeffries and Snyder 1981). Major sources of heavy metals in rainwater samples are fossil fuel combustion, motor vehicle pollution, mining, and forest fire along with dust particles which originate from non-protected areas in the land due to erosion of sedimentary rocks (Farahmandkia et al. 2010; Sabuti and Mohamed 2016). Furthermore, the concentration of trace metals in rainwater was controlled by the closeness to the contributing source, wind direction (direction of air masses), the amount of precipitation, and first-day rainfall in the region after long period of dryness (Al-Khashman 2009; Koulousaris et al. 2009). However, in LRB, trace metal concentration in rainfall was contributed by petro-chemical (offshore stations) and other industrial activities, heavy use of fossil fuel, forest burning, shipping activity in the South China Sea, and soil dust from local areas due to non-protected nature of interior roads in the forest region (logging roads) along with those carried by long-distance flowing regional monsoon winds.

Comparison of rainwater chemical characteristics

An attempt has been also made to compare the rainwater chemical characteristics of LRB with selected areas in the world. For that, results of the studies carried out in Brazil, Indonesia, Jordan, the USA, South Korea, England, China, and India were extracted from numerous research publications (Table 4). It was also noted that most of the studies do not consider all the physico-chemical parameters considered in the present research. Considering the mean pH and EC, LRB showed higher values than all other places except

Table 4 Comparison of mean concentration of physico-chemical parameters in rainwater samples in LRB with selected locations in the world

Parameters	Limbang River Basin, Borneo	Juiz de Fora City, Brazil	Bandung City, Indonesia	Ghore El-Safi, Jordan	Newark, New Jersey, US	GIST campus, Gwangju, Korea	Thames river, South eastern England	Nanping Mangdang Mountain, China	Palampur Dist., Himachal Pradesh, India
pH	6.01	5.77	4.67	6.91	4.57	5.78	6.13	4.81	6.11
EC (µS/cm)	90.85	11.30	17.79	95	-	27.82	48.5	20.01	33.62
TDS (mg/L)	63.60	-	-	-	-	-	-	-	-
DO (mg/L)	6.87	-	-	-	-	-	-	-	-
Turbidity (NTU)	0.91	-	-	-	-	-	-	-	-
Bicarbonate (mg/L)	32.01	1.80	-	8.153	-	-	-	-	-
Chloride (mg/L)	28.02	0.614	0.292	5.053	1.08	4.4	7.925	0.205	15.30
Ca (mg/L)	0.97	0.792	0.684	3.3064	0.21	0.7	3.29	0.605	3.95
Mg (mg/L)	0.37	0.289	0.060	1.117	0.05	0.2	0.565	0.074	0.14
Na (mg/L)	1.87	0.575	0.114	3.003	0.60	1.4	3.85	0.163	0.2
K (mg/L)	0.35	0.278	0.233	3.3232	0.06	0.3	0.405	0.208	0.9
Co (mg/L)	0.024	-	0.006	0.43	0.00002	-	0.00155	0.00005	-
Ni (mg/L)	0.138	-	0.0059	0.003	0.0055	0.00028	0.00405	0.001	0.183
Cd (mg/L)	0.005	BDL	0.0057	0.052	0.00003	0.00009	-	-	0.00022
Fe (mg/L)	1.054	-	0.0348	0.43	0.00835	0.011	0.019	0.0153	-
Mn (mg/L)	0.029	-	-	-	-	0.00458	0.01365	0.0062	-
Pb (mg/L)	0.037	BDL	0.0767	0.066	0.00047	0.00310	0.0012	0.0096	0.00385
Zn (mg/L)	0.015	0.007	0.0335	0.21	0.00660	0.01878	0.1231	0.065	-
Cu (mg/L)	0.012	0.004	0.0088	0.073	0.00282	0.00169	0.00245	0.0038	0.0011
Reference	Present study	Cerqueira et al. (2014).	Hasan et al. (2017).	Al-Khashman (2009).	Song and Gao (2009).	Chon et al. (2015).	Neal et al. (2004)	Cheng et al. (2011)	Singh (2011)

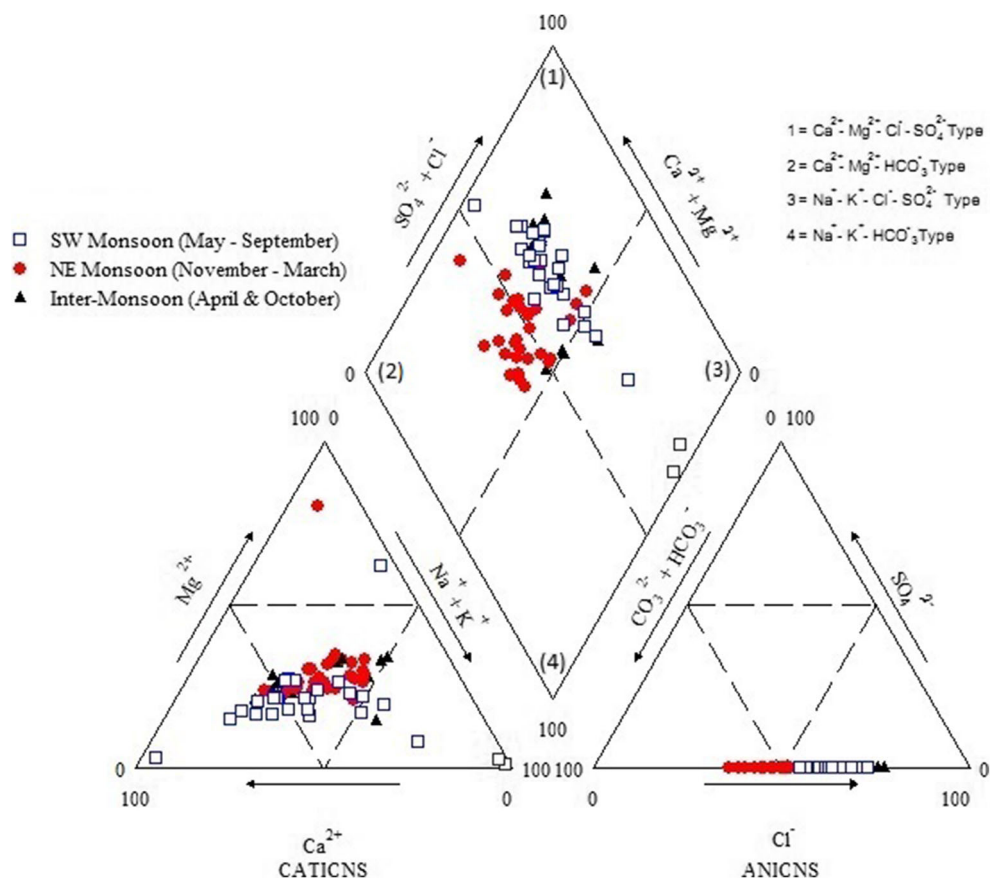
Jordan. Most locations are shown acidic nature of rainwater except Jordan. Higher value of EC in LRB indicates the presence of more suspended particulate matter in the atmosphere and rainwater. In the case of major cation concentration, rainwater in LRB showed moderate concentration but rainwater of England and India showed higher concentration. This indicates comparatively higher input of major ions from sea, land, and anthropogenic activities in those regions. At the same time, trace metals in rainwater collected from LRB shown lower concentration than Indonesia and Jordan. However, considering the concentration of trace metals in the region and comparing with the industrial development in the study area (region), trace metal shows higher concentration than industrially highly developed countries. Contribution of trace metals in the region can be ascribed to the monsoon winds originate from long-distance, presence of petro-chemical industries in the region, especially in the South China Sea and regional forest fire (biomass burning) in Southeast Asia. The comparison of rainwater chemistry of LRB with spatially and regionally separated locations in the world indicates that the

rainwater in LRB is also polluted due to the anthropogenic activities in the region.

Chemical classification of rainwater

Trilinear Piper diagram was used to determine the chemical facies of rainwater collected from LRB (Fig. 4). Piper plot revealed three major types of chemical facies, indicating three different sources which control the chemical characteristics of rainwater. During NEM, most of the rainwater samples fall in the $Ca^{2+}-Mg^{2+}-HCO_3^-$ facies and very less number of samples have shown mixed $Ca^{2+}-Mg^{2+}-Cl^-$ characteristics. Rainwater collected during the SWM has shown dominance of mixed $Ca^{2+}-Mg^{2+}-Cl^-$ facies with very few samples shown $Na^+-K^+-Cl^-$ characteristics. It was also noted that rainwater samples collected during inter-monsoon (IM) periods showed mixed $Ca^{2+}-Mg^{2+}-Cl^-$ facies. Though the seasonal rainwater samples have shown dominance of Ca^{2+} and Mg^{2+} in all the seasons, along with HCO_3^- , Cl^- , Na^+ and K^+ suggest variation in the source contribution of chemical constituents of

Fig. 4 Piper diagram showing the dominant water types (chemical facies) in rainwater samples collected from LRB



rainwater with respect to separate seasons (Sultan 2012). The possible source contribution of each major ion in the rainwater samples is detailed in the section chemical composition of rainwater.

Statistical analysis of rainwater

Correlation

Pearson's correlation test was carried out to find out the inter-relationship between the parameters. Season-wise analysis of correlation revealed a strong negative and positive correlation ($r \geq \pm 0.70$, significance level $\alpha = 0.05$) between the parameters and is discussed in the following sections. In NEM, moderate and good correlation was noted among the parameters (Table 5). pH has shown a strong correlation with DO ($r = 0.71$). EC showed a strong positive correlation with TDS and HCO_3^- ($r = 1, 0.98$) and a strong negative correlation with Fe ($r = -0.72$). TDS was positively (strong) correlated with HCO_3^- ($r = 0.98$) and negatively correlated with Fe ($r = -0.72$). HCO_3^- has shown a strong negative correlation with Na^+ and Fe ($r = -0.74$ and -0.75) and a strong positive correlation with Ni ($r = 0.71$). Ca^{2+} in the rainwater samples has shown a strong positive correlation with Na^+ , Cd, Fe, and Pb

($r = 0.85, 0.86, 0.83$, and 0.77). A strong positive correlation was found between Na^+ with Cd, Fe, Pb, and Zn ($r = 0.86, 0.87, 0.92$, and 0.70 respectively) and a strong negative correlation with Ni ($r = -0.74$). Co has shown a strong positive correlation with Cd and Fe ($r = 0.71$ and 0.70). Cd has shown a strong positive correlation with Fe and Pb ($r = 0.86$ and 0.77). Fe showed a strong positive correlation with Pb ($r = 0.88$). Pb shows strong correlation with Zn ($r = 0.75$).

However, during SWM, parameters in rainwater do not show much correlation like that observed in NEM (Table 6). During this season, EC showed a strong positive correlation with TDS, HCO_3^- , Cl^- , Na^+ , and K^+ ($r = 1, 0.82, 0.87, 0.93$, and 0.92 respectively). TDS showed a strong positive correlation with HCO_3^- , Cl^- , Na^+ , and K^+ ($r = 0.82, 0.87, 0.93$, and 0.92). A strong positive correlation was observed between Cl^- with Na^+ and K^+ ($r = 0.85$ and 0.84). Furthermore, Na^+ showed a strong positive correlation with K^+ ($r = 0.98$). Furthermore, examining the inter-monsoon (IM) period, parameters showed relatively higher correlation than those observed in SWM (Table 7). During this season, EC has shown strong positive correlation with TDS, HCO_3^- and Cl^- ($r = 1, 0.87$, and 0.94); a strong negative correlation with Mg^{2+} , Cd, Fe, Pb, Zn, and Cu ($r = -0.86, -0.78, -0.75, -0.86, -0.91$, and -0.71 respectively). A similar nature of correlation was observed between TDS with HCO_3^- and Cl^- ($r = 1, 0.87$, and

Table 5 Pearson’s correlations matrix for the physico-chemical parameters in NEM samples

	pH	EC (µS/cm)	TDS (mg/L)	DO (mg/L)	Turbidity (NTU)	Bicarbonate (mg/L)	Chloride (mg/L)	Ca (mg/L)	Mg (mg/L)	Na (mg/L)	K (mg/L)	Co (mg/L)	Ni (mg/L)	Cd (mg/L)	Fe (mg/L)	Mn (mg/L)	Pb (mg/L)	Zn (mg/L)	Cu (mg/L)	
pH	1																			
EC (µS/cm)	-0.39	1																		
TDS (mg/L)	-0.39	1.00	1																	
DO (mg/L)	0.71	-0.41	-0.41	1																
Turbidity(NTU)	0.20	0.13	0.13	0.22	1															
Bicarbonate (mg/L)	-0.48	0.98	0.98	-0.49	0.04	1														
chloride (mg/L)	0.32	-0.14	-0.14	0.29	0.23	-0.32	1													
Ca (mg/L)	0.66	-0.61	-0.61	0.65	0.13	-0.68	0.20	1												
Mg (mg/L)	0.31	-0.22	-0.22	0.25	0.00	-0.26	-0.04	0.30	1											
Na (mg/L)	0.68	-0.66	-0.66	0.67	0.30	-0.74	0.22	0.85	0.37	1										
K (mg/L)	0.17	0.13	0.13	-0.14	0.51	0.07	0.09	0.05	-0.08	0.33	1									
Co (mg/L)	0.42	-0.66	-0.66	0.28	0.05	-0.67	0.11	0.65	0.21	0.58	0.12	1								
Ni (mg/L)	-0.30	0.66	0.66	-0.33	-0.34	0.71	-0.24	-0.55	-0.31	-0.74	-0.24	-0.37	1							
Cd (mg/L)	0.49	-0.62	-0.62	0.43	0.20	-0.66	0.10	0.86	0.31	0.86	0.24	0.71	-0.58	1						
Fe (mg/L)	0.53	-0.72	-0.72	0.44	-0.02	-0.75	0.03	0.83	0.43	0.87	0.18	0.70	-0.61	0.86	1					
Mn (mg/L)	0.17	0.16	0.16	-0.08	-0.19	0.18	-0.19	0.13	-0.18	-0.05	0.21	0.12	0.25	-0.03	0.15	1				
Pb (mg/L)	0.57	-0.60	-0.60	0.58	0.22	-0.65	0.07	0.77	0.35	0.92	0.31	0.57	-0.61	0.77	0.88	0.05	1			
Zn (mg/L)	0.41	-0.49	-0.49	0.43	0.25	-0.55	0.23	0.65	0.17	0.70	0.15	0.48	-0.38	0.65	0.69	-0.03	0.75	1		
Cu (mg/L)	-0.24	0.27	0.27	-0.05	0.00	0.29	-0.12	-0.14	-0.09	-0.18	-0.17	-0.22	0.25	-0.08	-0.22	-0.04	-0.05	0.08	1	

Values in bold are different from 0 with a significance level alpha=0.05; bold values indicate r≥±0.70

0.94), a strong negative correlation with Mg²⁺, Cd, Fe, Pb, Zn, and Co (*r* = -0.86, -0.78, -0.75, -0.86, -0.91, and -0.71 respectively). HCO₃⁻ in the rainwater has shown a strong negative correlation with Mg²⁺ and Pb (*r* = -0.82 and -0.76). A strong negative correlation exists between Cl⁻ with Mg²⁺, Cd, Fe, Pb, Zn, and Cu (-0.87, -0.78, -0.76, -0.81, -0.94, and -0.78 respectively). Mg²⁺ showed a strong positive correlation with Na⁺, Cd, Fe, and Pb (*r* = -0.81, 0.94, 0.93, and 0.95). The positive correlation observed between Na⁺ with Fe and Pb is strong (*r* = 0.75 and 0.73). Cd has shown a strong positive correlation with Fe, Pb, Zn, and Cu (*r* = 0.93, 0.88, 0.70, and 0.70 respectively). Fe has shown positive strong correlation with Pb (*r* = 0.90). A strong positive correlation was observed between Pb and Zn (*r* = 0.72), whereas Zn has shown a strong positive correlation with Cu (*r* = 0.79)

The correlation analysis explained inter-relationship (both positive and negative) between different physico-chemical parameters present in the rainwater collected from LRB during different seasons. Strong positive correlation between the

variable generally indicates same source of origin, i.e., either marine or continental, whereas the negative correlation indicates the concentration of one parameter control the dominance of the parameter (Al-Hashman 2009). Furthermore, it was also noted that some parameters do not show correlation suggesting a different source of origin (Khatoun et al. 2013). In the present research, the observed change in the correlation between the parameters during different seasons suggests variation in source contribution of rainfall along with local input in the moisture source of rainwater collected at spatially separated but unique rainfall regime of LRB.

ANOVA

Analysis of variance (two-way ANOVA) was conducted to understand the variation in values, and the concentration of parameters between sampling locations and seasons because the analysis of variance (ANOVA) is capable of expressing the variation between and within the group of samples (Dominique et al. 1998; Calabrese et al. 2015). Two-way

Table 6 Pearson’s correlations matrix for the physico-chemical parameters in SWM samples

Variables	pH	EC (µS/cm)	TDS (mg/L)	DO (mg/L)	Turbidity (NTU)	Bicarbonate (mg/L)	Chloride (mg/L)	Ca (mg/L)	Mg (mg/L)	Na (mg/L)	K (mg/L)	Co (mg/L)	Ni (mg/L)	Cd (mg/L)	Fe (mg/L)	Mn (mg/L)	Pb (mg/L)	Zn (mg/L)	Cu (mg/L)	
pH	1																			
EC (µS/cm)	0.13	1																		
TDS (mg/L)	0.13	1.00	1																	
DO (mg/L)	0.02	0.28	0.28	1																
Turbidity(NTU)	0.11	0.43	0.43	0.21	1															
Bicarbonate (mg/L)	0.40	0.82	0.82	0.27	0.42	1														
Chloride (mg/L)	-0.14	0.87	0.87	0.17	0.25	0.52	1													
Ca (mg/L)	0.42	0.18	0.18	0.15	-0.17	0.40	-0.13	1												
Mg (mg/L)	0.40	0.05	0.05	0.22	0.63	0.22	-0.17	-0.03	1											
Na (mg/L)	-0.01	0.93	0.93	0.23	0.47	0.62	0.85	-0.08	0.05	1										
K (mg/L)	-0.06	0.92	0.92	0.29	0.48	0.59	0.84	-0.05	0.02	0.98	1									
Co (mg/L)	0.25	0.13	0.13	0.27	-0.16	0.17	0.07	0.26	-0.15	0.04	0.01	1								
Ni (mg/L)	-0.14	-0.10	-0.10	0.20	-0.24	-0.19	-0.08	0.18	-0.37	-0.07	-0.06	0.20	1							
Cd (mg/L)	0.40	0.04	0.04	-0.12	-0.05	0.22	-0.01	0.17	-0.20	-0.08	-0.07	0.04	0.17	1						
Fe (mg/L)	-0.34	-0.38	-0.38	0.24	-0.25	-0.21	-0.30	0.00	-0.34	-0.44	-0.41	0.10	0.35	-0.12	1					
Mn (mg/L)	-0.27	0.00	0.00	-0.26	0.01	0.16	0.06	-0.27	-0.26	-0.05	-0.03	0.06	-0.21	0.27	0.18	1				
Pb (mg/L)	0.64	-0.03	-0.03	-0.03	-0.01	0.09	-0.10	0.27	-0.02	-0.12	-0.13	0.37	0.06	0.51	-0.02	-0.03	1			
Zn (mg/L)	0.04	-0.31	-0.31	-0.08	-0.29	-0.37	-0.19	-0.10	0.04	-0.26	-0.32	0.08	0.10	0.05	-0.04	-0.37	0.03	1		
Cu (mg/L)	0.17	-0.28	-0.28	0.08	0.32	-0.03	-0.44	-0.13	0.49	-0.24	-0.24	-0.23	-0.19	0.06	0.12	0.16	0.22	0.02	1	

Values in bold are different from 0 with a significance level alpha=0.05; bold values indicate r≥±0.70

Table 7 Pearson’s correlations matrix for the physico-chemical parameters in IM samples

Variables	pH	EC (µS/cm)	TDS (mg/L)	DO (mg/L)	Turbidity (NTU)	Bicarbonate (mg/L)	Chloride (mg/L)	Ca (mg/L)	Mg (mg/L)	Na (mg/L)	K (mg/L)	Co (mg/L)	Ni (mg/L)	Cd (mg/L)	Fe (mg/L)	Mn (mg/L)	Pb (mg/L)	Zn (mg/L)	Cu (mg/L)	
pH	1																			
EC (µS/cm)	0.15	1																		
TDS (mg/L)	0.15	1.00	1																	
DO (mg/L)	0.65	-0.04	-0.04	1																
Turbidity(NTU)	0.51	0.11	0.11	0.00	1															
Bicarbonate (mg/L)	0.24	0.87	0.87	-0.22	0.35	1														
Chloride (mg/L)	0.04	0.94	0.94	0.06	-0.05	0.65	1													
Ca (mg/L)	0.07	-0.44	-0.44	0.37	-0.43	-0.65	-0.25	1												
Mg (mg/L)	-0.04	-0.86	-0.86	0.33	-0.20	-0.82	-0.78	0.55	1											
Na (mg/L)	0.14	-0.66	-0.66	0.35	-0.26	-0.63	-0.63	0.58	0.81	1										
K (mg/L)	-0.08	-0.52	-0.52	0.06	0.07	-0.37	-0.54	-0.34	0.48	0.41	1									
Co (mg/L)	-0.27	-0.13	-0.13	-0.40	0.23	-0.06	-0.15	0.13	-0.08	-0.05	-0.32	1								
Ni (mg/L)	-0.13	-0.13	-0.13	-0.49	-0.15	0.24	-0.36	-0.13	-0.02	-0.04	-0.09	-0.04	1							
Cd (mg/L)	0.01	-0.78	-0.78	0.21	-0.05	-0.65	-0.78	0.41	0.94	0.69	0.44	-0.18	0.167	1						
Fe (mg/L)	0.02	-0.75	-0.75	0.28	-0.06	-0.60	-0.76	0.27	0.93	0.75	0.61	-0.15	0.07	0.93	1					
Mn (mg/L)	-0.31	-0.23	-0.23	-0.05	-0.58	-0.20	-0.26	0.32	0.42	0.67	0.12	0.11	0.24	0.32	0.45	1				
Pb (mg/L)	0.17	-0.86	-0.86	0.41	0.01	-0.76	-0.81	0.49	0.95	0.73	0.45	0.00	-0.05	0.88	0.90	0.25	1			
Zn (mg/L)	-0.11	-0.91	-0.91	-0.19	-0.01	-0.66	-0.94	0.35	0.68	0.46	0.32	0.20	0.44	0.70	0.60	0.12	0.72	1		
Cu (mg/L)	0.01	-0.71	-0.71	-0.20	-0.05	-0.47	-0.78	0.45	0.62	0.67	0.22	0.05	0.48	0.70	0.55	0.37	0.54	0.79	1	

Values in bold are different from 0 with a significance level alpha=0.05; bold values indicate $r \geq \pm 0.70$

ANOVA statistics revealed significant (95% confidence level or $p \leq 0.05$) relationships between the parameters and variables considered (Table 8). Among the parameters, Ni, Fe, and Cu have shown statistically significant variation between sampling locations and sampling seasons. Parameters such as pH, EC, TDS, DO, HCO_3^- , Cl^- , Co, Cd, Mn, Pb, and Zn have shown statistically significant variation between the sampling periods, whereas turbidity and K^+ have shown statistically significant variation between the sampling locations. Ca^{2+} , Mg^{2+} , and Na^+ showed no significant variation between sampling locations and sampling periods.

Factor analysis

Principal component analysis (PCA)-based factor extraction was carried out in the results of physico-chemical parameters of rainwater collected in each season to identify the source of ions in rainwater samples with an Eigenvalue larger than 1, after varimax rotation. Varimax rotation will make the interpretation of results easier by minimizing the variance of squared normalized factor loadings across variables for each factor (Báez et al. 2007). Results of the factor analysis are shown in Table 9. In NEM, factor analysis revealed three factors which explained 79.80% of total variance. Factor 1 explained 45.66% of total variance with high loading for EC, TDS, and HCO_3^- . EC and TDS are physical parameters which are contributed by the suspended particles in the atmosphere originated from natural and anthropogenic activities (Rusydi 2018). HCO_3^- in rainwater in this region was contributed by the increased amount of CO_2 in the atmosphere due to forest fires as well as the soil dust rich in carbonate contents formed by anthropogenic activities (Hu et al. 2003). Factor 2 explained 21.76% of the total variance with strong loading of

K^+ and moderate loading of pH, Na^+ , Ca^{2+} and weak loading of Cl^- . This explained concentration of K^+ in rainwater is mainly from biomass burning. Na^+ and Cl^- indicate marine contribution and are due to the presence of aerosols and evaporation-based sea salt in the atmosphere and Ca^{2+} might be originated from dust particles evolved from calcareous soil (Tsukuda et al. 2006; Cerqueira et al. 2014). Factor 3 explained 12.38% of total variance with strong loading of Mg^{2+} , might be contributed by sea and land, as evaporation of saltwater or due to the influence of dispersion of soil and biological fragments and excess emission of alkaline dust in rainwater (De Mello 2001; Al-Khashman 2009).

Considering SWM, three factors identified explained a cumulative variance of 90.72%. Factor 1 explained 57.18% of total variance by strong loading of EC, TDS, Na^+ , K^+ , Cl^- , and HCO_3^- . This indicates the dominance of suspended particulate matter, biomass burning in the region, evaporation of sea salt, and an increased amount of CO_2 in the atmosphere due to forest fires as well as the soil dust rich in carbonate content in the atmosphere (Shrestha et al. 2013). Factor 2 explained 18.44% of the total variance with strong loading of Ca^{2+} and moderate loadings of HCO_3^- and pH, suggesting dominance of calcareous dust particles, forest fire, and biomass burning induced CO_2 concentration in the atmosphere along with carbonate rich soil dust evolved from the region (Lewis Jr. 1981; Shrestha et al. 2013). Factor 3 explained 15.10% of the total variance with strong loading of Mg^{2+} and moderate loading of pH. This explains the dispersion of soil and biological fragments and excess emission of alkaline dust in rainwater (De Mello 2001; Al-Khashman 2009). At the same time, in IM, season factor analysis revealed three factor components which explained cumulative variance of 90.52%. Factor 1 explained 61.84% of the total variance with strong

Table 8 Two-way ANOVA of rainwater quality parameters of LRB

		% of total variation	SS	MS	F	p value	Significance
pH	Between stations	0.035	0.422	0.084	0.563	0.728	No
	Between months	0.287	3.486	0.317	2.115	0.034	Yes
EC (µS/cm)	Between stations	0.044	3222.758	644.552	1.369	0.250	No
	Between months	0.603	44160.654	4014.605	8.526	0.000	Yes
TDS (mg/L)	Between stations	0.044	1579.152	315.830	1.369	0.250	No
	Between months	0.603	21638.720	1967.156	8.526	0.000	Yes
DO (mg/L)	Between stations	0.050	5.749	1.150	0.995	0.429	No
	Between months	0.397	45.544	4.140	3.584	0.001	Yes
Turbidity (NTU)	Between stations	0.298	20.435	4.087	6.051	0.000	Yes
	Between months	0.161	11.075	1.007	1.491	0.162	No
Bicarbonate (mg/L)	Between stations	0.033	178.756	35.751	0.956	0.452	No
	Between months	0.584	3136.787	285.162	7.629	0.000	Yes
Chloride (mg/L)	Between stations	0.011	125.968	25.194	0.865	0.510	No
	Between months	0.845	9443.532	858.503	29.482	0.000	Yes
Ca (mg/L)	Between stations	0.068	18.419	3.684	1.025	0.412	No
	Between months	0.206	56.043	5.095	1.418	0.191	No
Mg (mg/L)	Between stations	0.061	0.910	0.182	0.899	0.488	No
	Between months	0.190	2.825	0.257	1.269	0.267	No
Na (mg/L)	Between stations	0.127	312.884	62.577	1.900	0.109	No
	Between months	0.137	336.121	30.556	0.928	0.521	No
K (mg/L)	Between stations	0.152	8.870	1.774	2.463	0.044	Yes
	Between months	0.167	9.746	0.886	1.230	0.290	No
Co (mg/L)	Between stations	0.021	0.000	0.000	0.744	0.594	No
	Between months	0.667	0.009	0.001	10.684	0.000	Yes
Ni (mg/L)	Between stations	0.041	0.007	0.001	3.471	0.008	Yes
	Between months	0.829	0.140	0.013	31.940	0.000	Yes
Cd (mg/L)	Between stations	0.050	0.00	0.000	2.315	0.056	No
	Between months	0.712	0.0002	0.000	14.990	0.000	Yes
Fe (mg/L)	Between stations	0.057	0.297	0.059	2.902	0.021	Yes
	Between months	0.727	3.786	0.344	16.817	0.000	Yes
Mn (mg/L)	Between stations	0.069	0.000	0.000	1.430	0.228	No
	Between months	0.400	0.002	0.000	3.769	0.000	Yes
Pb (mg/L)	Between stations	0.008	0.000	0.000	0.616	0.688	No
	Between months	0.854	0.045	0.004	30.908	0.000	Yes
Zn (mg/L)	Between stations	0.012	0.000	0.000	0.394	0.851	No
	Between months	0.644	0.005	0.000	9.358	0.000	Yes
Cu (mg/L)	Between stations	0.095	0.000	0.000	3.813	0.005	Yes
	Between months	0.630	0.001	0.000	11.466	0.000	Yes

loading of EC, TDS, HCO₃⁻, and Cl⁻. This is due to the dominance of suspended particulate matter, evaporation of sea salt, and increased amount of CO₂ in the atmosphere due to forest fires as well as the soil dust rich in carbonate content in the atmosphere (Shrestha et al. 2013). Factor 2 explained 16.11% of the total variance by strong loading of Ca²⁺ (De Mello 2001). Factor 3 explained 12.56% of total variance with strong loading pH.

Overall, it can be concluded that rainwater chemistry in LRB was controlled by natural as well as anthropogenic

processes, but the variation of water chemistry between the seasons was observed. Factor analysis facilitated the identification of major processes which controls the chemistry of rainwater in the region and are (a) contribution of soil dust through wind and sea salt through evaporation, (b) anthropogenic pollution-based factors such as fossil fuel burning (petro-chemical industries and transportation) and forest fire in the region as well as that carried from long distance by cloud winds, and (c) vehicle emission. It was also noted that contribution of these factors also varies between season to

Table 9 Results of factor analysis of physico-chemical parameters in rainwater samples of different season in LRB

Parameters	NEM			SWM			IM		
	Factor 1	Factor 2	Factor 3	Factor 1	Factor 2	Factor 3	Factor 1	Factor 2	Factor 3
pH	-0.43	0.69	0.13	-0.01	0.64	0.58	0.06	0.04	0.97
EC	0.98	-0.01	-0.03	0.98	0.19	0.05	0.97	0.04	0.13
TDS	0.98	-0.01	-0.03	0.98	0.19	0.05	0.97	0.04	0.13
HCO ₃	0.98	-0.16	0.04	0.72	0.52	0.25	0.88	-0.25	0.24
Cl	-0.24	0.39	-0.62	0.92	-0.13	-0.18	0.90	0.21	0.00
Ca	-0.68	0.51	0.19	-0.01	0.94	-0.10	-0.51	0.85	0.08
Mg	-0.22	0.23	0.78	0.01	-0.04	0.95	-0.94	0.09	0.04
Na	-0.66	0.67	0.18	0.97	-0.09	0.05	-0.81	0.15	0.31
K	0.27	0.74	-0.16	0.96	-0.09	0.00	-0.56	-0.76	0.01
% of variance explained	45.66	21.76	12.38	57.18	18.44	15.102	61.84	16.11	12.56
Cumulative % of variance	79.80			90.72			90.52		

Bold italic values indicate strong loading

season, i.e., NEM, SWM, and IM seasons. Though these are the major factors controlling the chemical characteristics of rainwater in the region, specific characteristics of location and the local addition of natural and anthropogenic processes have influenced the variation in chemical characteristics in different seasons. These points towards the movement of air pollutants in the region, which was controlled by wind blowing over the region.

In order to confirm the variation in source contribution of chemical constituents reaching LRB, backward air mass trajectory corresponding to the study period was generated using a HYSPLIT transport model. Backward trajectory analysis is the best available tool in air quality and pollutant movement modeling which helps to generate a comprehensive information about the origins and sources of pollutants in the atmosphere as well as which reaching the surface through rainfall

(Chen et al. 2013; Tatsuta et al. 2017; Tu et al. 2019). In the present research, individual season representation was considered to build the backward air mass trajectory, and results were interpreted. For the HYSPLIT analysis, the months of January 2017 (NEM), August 2017 (SWM), and April 2017 (IM period) were selected and modeled at three different heights, i.e., 500, 1000, and 1500 m above ground level (Fig. 5). It was observed that, during NEM season (Fig. 5a), the pollutants are reaching the study area from the north and east directions and show a mixed contribution, i.e., from the ocean (the South China Sea) and land area with dominance of land contribution. A contrasting characteristic was observed during SWM season (Fig. 5b), which shows dominance of west and southwest direction with less contribution from land and major contribution from the ocean. However, considering the IM season (Fig. 5c), the study area received dominant

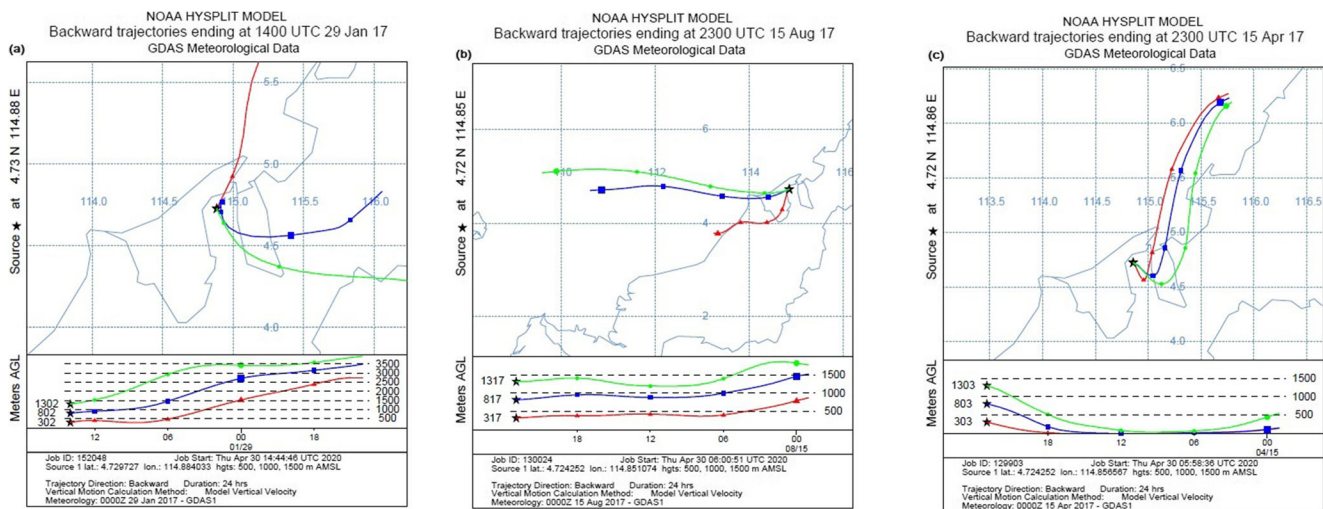


Fig. 5 Samples of air mass backward trajectories reaching LRB during (a) NEM season (b) SWM season, and (c) IM season at 500, 1000, and 1500 m above ground level

pollutant load from north, northeast direction with sole contribution from ocean source (the South China Sea). This confirms the variability in seasonal rainwater chemical characteristic explained by statistical methods and control of land- and ocean-based pollutants over the rainwater chemistry of LRB.

Enrichment factors

In order to understand the source of ionic contribution in the rainwater reaching LRB, the enrichment factors for sea water and crust were estimated. In most studies Na, Al, and Ca²⁺ were taken as reference elements to estimate the marine and crustal contribution because Na⁺ is considered of purely marine origin, whereas Al and Ca²⁺ are lithogenic, i.e., originate from continental crust (Keene et al. 1986; Kulshrestha et al. 2003; Zhang et al. 2007; Cao et al. 2009). Source contribution of ionic components in rainwater samples collected from LRB was estimated by considering Na⁺ and Ca²⁺ as the reference element for marine and crustal sources. The enrichment factor was calculated using the equations:

$$EF_{\text{marine}} = \frac{[X/Na^+]_{\text{rainwater}}}{[X/Na^+]_{\text{seawater}}} \tag{1}$$

$$EF_{\text{crust}} = \frac{[X/Ca^{2+}]_{\text{rainwater}}}{[X/Ca^{2+}]_{\text{soil}}} \tag{2}$$

where *X* is the concentration of ion or element of interest in rainwater, *X*/Na⁺ is the proportion of seawater composition, and *X*/Ca²⁺ is the proportion of crustal composition.

Enrichment factor analysis of seasonal rainwater samples of different seasons has shown similar characteristics with slight variation in the enrichment of individual elements with higher values (> 1) (Zhang et al. 2007; Lu et al. 2011) (Table 10). During NEM, except K⁺, all elements show source from both marine and crust, whereas K⁺ has shown purely crustal origin with EF_{crust} value of 0.47. Considering SWM,

Cl⁻ and Ca²⁺ show mixed source origin with comparatively higher values in EF_{seawater} and EF_{crust} ratio. Low ratio found for Mg²⁺ (0.45 and 0.44) indicates almost equal contribution of marine and crustal source, whereas the K⁺ was solely contributed from crustal source (EF_{crust} ratio is 0.90). During IM period, a similar source contribution was observed with K⁺ originated from a crustal source (EF_{crust} ratio is 0.47) and Mg²⁺ from a mixed source, i.e., mostly from crustal and partially from marine (EF_{seawater} and EF_{crust} ratio is 1.68 and 0.86 respectively). The crustal enrichment of ions observed indicates that the source contribution from crustal source also comprises certain contribution from anthropogenic activities.

Conclusion

Chemical characteristics of seasonal rainwater in the equatorial tropical rainforest region in northwestern Borneo indicate varying characteristics suggesting variation in source and contribution from local areas. Rainwater in all seasons (NEM, SWM, and IM periods) has shown slightly alkaline nature (mean pH > 5.8) against the neutral pH of cloud water (5.6) with atmospheric CO₂ equilibrium. Moderate values of EC and TDS in rainwater samples indicate the presence of suspended particulate matter indicating slightly polluted atmospheric environment over LRB. Seasonal rainfall in LRB has shown slight variation in concentration of major ions but chloride and HCO₃⁻ as dominant ions in all seasons. Abundance of trace metals such as Co, Ni, Cd, Fe, Mn, Pb, Zn, and Cu was measured in rainwater samples in which Fe, Ni, Pb, Mn, and Co have shown comparatively higher concentrations in all the seasons. Hydrochemical facies analysis and factor analysis indicate variation in source contribution of chemical characteristics of rainwater in LRB. Two-way ANOVA analysis backs up the findings by showing significant variation in chemical characteristics between seasons and sampling locations. Pearson’s correlation analysis also indicates the same results by identifying varying correlation between the parameters analyzed in rainwater during NEM, SWM, and IM periods. The enrichment factor analysis suggests contribution of mixed source, i.e., marine and crustal sources in the chemical characteristics of rainwater in LRB. Backward air mass trajectory analysis by a HYSPLIT transport model also confirms the same with seasonal variation in source contribution. It can be concluded that the seasonal variation in chemical characteristic of rainwater in LRB is controlled by natural as well as anthropogenic processes operating in the region. The plausible dominant processes which contribute the chemical constituents to rainwater are petrochemical and industrial activities, fossil fuel combustion, forest burning and forest fire, shipping activity in the South China Sea, and soil dust from non-protected logging roads along with those carried by regional seasonal winds.

Table 10 Source contributions for different ionic constituents in rainwater samples of different seasons in LRB

Seasons	Enrichment factor	Cl ⁻	K ⁺	Mg ²⁺	Ca ²⁺	Na ⁺
NEM	EF _{seawater}	19.42	9.22	2.30	19.43	-
	EF _{crust}	8473.27	0.47	1.08	-	2.06
SWM	EF _{seawater}	10.16	8.50	0.45	9.41	-
	EF _{crust}	9153.09	0.90	0.44	-	4.25
IM	EF _{seawater}	22.38	8.50	1.68	17.93	-
	EF _{crust}	10584.71	0.47	0.86	-	2.23

Acknowledgments The authors gratefully acknowledge the Department of Irrigation and Drainage (DID), Sarawak, Malaysia for providing rainfall data. Authors are also thankful to the Managing Editor Dr. Philippe Garrigues and anonymous reviewers for their critical reviews, constructive comments, and suggestions, which significantly improved the quality of the manuscript.

Funding information The first author was provided financial support from the Curtin University Malaysia (CMPRS) and research facility during the study.

References

- Abulude F, Ndamitso MM, Abdulkadir A (2018) Environmental situation of an agricultural area in Akure, Nigeria, based on physico-chemical properties of rainwater. *Pollution* 4(2):317–325
- Adugna D, Jensen MB, Lemma B, Gebrie GS (2018) Assessing the potential for rooftop rainwater harvesting from large public institutions. *Int J Environ Res Public Health* 15(2):336
- Akpan AO, Udosen ED, Offiong NAO (2018) Rainwater chemistry within the vicinity of Qua Iboe Estuary, Nigeria. *CLEAN–Soil Air Water* 46(3):1700114
- Al Obaidy AHMJ, Joshi H (2006) Chemical composition of rainwater in a tropical urban area of northern India. *Atmos Environ* 40(35):6886–6891
- Al-Khashman OA (2009) Chemical characteristics of rainwater collected at a western site of Jordan. *Atmos Res* 91(1):53–61
- Al-Khlaifat AL, Al-Khashman OA (2007) Atmospheric heavy metal pollution in Aqaba city, Jordan, using Phoenix dactylifera L. leaves. *Atmos Environ* 41(39):8891–8897
- American Public Health Association (APHA) (1995) Standard methods for the examination of water and wastewater. 19th ed. Byrd Prepress Springfield, Washington
- American Public Health Association (APHA) (2012) Standard methods for the examination of water and waste water. 22nd ed. American Water Works Association, Water Environment Federation (APHA)
- Avila A, Alarcón M (1999) Relationship between precipitation chemistry and meteorological situations at a rural site in NE Spain. *Atmos Environ* 33(11):1663–1677
- Báez A, Belmont R, García R, Padilla H, Torres MDC (2007) Chemical composition of rainwater collected at a southwest site of Mexico City, Mexico. *Atmos Res* 86(1):61–75
- Baklanov A, Molina LT, Gauss M (2016) Megacities, air quality and climate. *Atmos Environ* 126:235–249
- Boubel RW, Fox DL, Turner DB, Stern AC (1994) Fundamentals of air pollution. United States: Academic Press.
- Brännvall ML, Bindler R, Renberg I, Emteryd O, Bartnicki J, Billström K (1999) The Medieval metal industry was the cradle of modern large-scale atmospheric lead pollution in northern Europe. *Environ Sci Technol* 33(24):4391–4395
- Calabrese F, Van Der Doelen RH, Guidotti G, Racagni G, Kozicz T, Homberg JR, Riva MA (2015) Exposure to early life stress regulates Bdnf expression in SERT mutant rats in an anatomically selective fashion. *J Neurochem* 132(1):146–154
- Calvo AI, Olmo FJ, Lyamani H, Alados-Arboledas L, Castro A, Fernández-Raga M, Fraile R (2010) Chemical composition of wet precipitation at the background EMEP station in Vézinar (Granada, Spain) (2002–2006). *Atmos Res* 96(2-3):408–420
- Cao YZ, Wang S, Zhang G, Luo J, Lu S (2009) Chemical characteristics of wet precipitation at an urban site of Guangzhou, South China. *Atmos Res* 94(3):462–469
- Corqueira MRF, Pinto MF, Derossi IN, Esteves WT, Santos MDR, Matos MAC, Lowinsohn D, Matos RC (2014) Chemical characteristics of rainwater at a southeastern site of Brazil. *Atmos Pollut Res* 5(2): 253–261
- Chambers SD, Wang F, Williams AG, Xiaodong D, Zhang H, Lonati G, Crawford J, Griffiths AD, Ianniello A, Allegrini I (2015) Quantifying the influences of atmospheric stability on air pollution in Lanzhou, China, using a radon-based stability monitor. *Atmos Environ* 107:233–243
- Chen B, Stein AF, Maldonado PG, Campa AM, Castaneda YG, Castell N, Rosa JD (2013) Size distribution and concentrations of heavy metals in atmospheric aerosols originating from industrial emissions as predicted by the HYSPLIT model. *Atmos Environ* 71:234–244
- Cheng S (2003) Heavy metal pollution in China: origin, pattern and control. *Environ Sci Pollut Res* 10(3):192–198
- Cheng Y, Liu Y, Huo M, Sun Q, Wang H, Chen Z, Bai Y (2011) Chemical characteristics of precipitation at Nanping Mangdang Mountain in eastern China during spring. *J Environ Sci (China)* 23(8):1350–1358
- Chon K, Kim Y, Bae DH, Cho J (2015) Confirming anthropogenic influences on the major organic and inorganic constituents of rainwater in an urban area. *Drinking Water. Eng Sci* 8(2):35–48
- Cobbina SJ, Michael K, Salifu L, Duwiewua AB (2013) Rainwater quality assessment in the Tamale municipality. *Int J Sci Technol Res* 2:1–10
- Cong Z, Kang S, Zhang Y, Li X (2010) Atmospheric wet deposition of trace elements to central Tibetan Plateau. *Appl Geochem* 25(9): 1415–1421
- Crutzen PJ, Andreae MO (1990) Biomass burning in the tropics: impact on atmospheric chemistry and biogeochemical cycles. *Science* 250(4988):1669–1678
- De Mello WZ (2001) Precipitation chemistry in the coast of the Metropolitan Region of Rio de Janeiro, Brazil. *Environ Pollut* 114(2):235–242
- Dominique JF, Roozendaal B, McLaugh JL (1998) Stress and glucocorticoids impair retrieval of long-term spatial memory. *Nature* 394(6695):787
- Durand P, Neal C, Lelong F (1992) Anthropogenic and natural contributions to the rainfall chemistry of a mountainous area in the Cevennes National Park (Mont-Lozere, southern France). *J Hydrol* 130(1-4): 71–85
- Farahmandkia Z, Mehrasbi MR, Sekhvatjou MS (2010) Relationship between concentrations of heavy metals in wet precipitation and atmospheric pm10 > particles in Zanjan, Iran. *Iran J Environ Health Sci Eng* 8(1):49–56
- Francová A, Chrástný V, Šillerová H, Vítková M, Kocourková J, Komárek M (2017) Evaluating the suitability of different environmental samples for tracing atmospheric pollution in industrial areas. *Environ Pollut* 220:286–297
- Galloway JN, Likens GE, Keene WC, Miller JM (1982) The composition of precipitation in remote areas of the world. *J Geophys Res Oceans* 87(C11):8771–8786
- Ghimire SR, Johnston JM, Ingwersen WW, Hawkins TR (2014) Life cycle assessment of domestic and agricultural rainwater harvesting systems. *Environ Sci Technol* 48(7):4069–4077
- Gomyo M, Kuraji K, Kitayama K, Suzuki M (2008) Rainfall, bulk deposition of nutrients and their seasonal variation in two tropical lowland and montane forests in Borneo. In AGU Fall Meeting Abstracts.
- Gordon AM, Chourmouzis C, Gordon AG (2000) Nutrient inputs in litterfall and rainwater fluxes in 27-year old red, black and white spruce plantations in Central Ontario, Canada. *For Ecol Manag* 138(1-3):65–78
- Graeff V, Mottin IG, Rocha-Urriarte L, Osório DMM, Schmitt JL (2018) Assessment of a subtropical riparian forest focusing on botanical, meteorological, ecological characterization and chemical analysis of rainwater. *Rev Ambiente Água* 13(2):e2140. <https://doi.org/10.4136/ambi-agua.2140>

- Hasan NY, Driejana D, Sulaeman A (2017) Composition of Ions and Trace Metals in Rainwater in Bandung City, Indonesia. *IPTEK J Proc Series* 3(6):603–608.
- Hu Y, Cheng H (2016) A method for apportionment of natural and anthropogenic contributions to heavy metal loadings in the surface soils across large-scale regions. *Environ Pollut* 214:400–409
- Hu GP, Balasubramanian R, Wu CD (2003) Chemical characterization of rainwater at Singapore. *Chemosphere* 51(8):747–755
- Jeffries DS, Snyder WR (1981) Atmospheric deposition of heavy metals in central Ontario. *Water Air Soil Pollut* 15(2):127–152
- Keene WC, Galloway JN (1986) Considerations regarding sources for formic and acetic acids in the troposphere. *J Geophys Res Atmos* 91(D13):14466–14474
- Keller M, Jacob DJ, Wofsy SC, Harriss RC (1991) Effects of tropical deforestation on global and regional atmospheric chemistry. *Clim Chang* 19(1-2):139–158
- Khatoun N, Khan AH, Rehman M, Pathak V (2013) Correlation study for the assessment of water quality and its parameters of Ganga River, Kanpur, Uttar Pradesh, India. *IOSR J Appl Chem* 5(3):80–90
- Khoo SH, Issabayeva GI, Lee LW (2011) Measurement of rainwater chemical composition in Malaysia based on ion chromatography method. *World Acad Sci Eng Technol* 11:161–168
- Komabayasi M (1959) Dissolved oxygen in rainwater and its relation to the raincloud structure (I). precipitation from September to March. *J Meteorol Soc Japan Ser II* 37(1):22–34
- Kord B, Kord B (2011) Heavy metal levels in pine (*Pinus sardarica* Medw.) tree barks as indicators of atmospheric pollution. *BioResources* 6(2): 927–935
- Koulousaris M, Aloupi M, Angelidis MO (2009) Total metal concentrations in atmospheric precipitation from the Northern Aegean Sea. *Water Air Soil Pollut* 201(1-4):389
- Kulshrestha UC, Kulshrestha MJ, Sekar R, Sastry GSR, Vairamani M (2003) Chemical characteristics of rainwater at an urban site of south-central India. *Atmos Environ* 37(21):3019–3026
- Kumar P, Yadav S, Kumar A (2014) Sources and processes governing rainwater chemistry in New Delhi, India. *Nat Hazards* 74(3):2147–2162
- Lee JY, Yang JS, Han M, Choi J (2010) Comparison of the microbiological and chemical characteristics of harvested rainwater and reservoir water as alternative water resources. *Sci Total Environ* 408(4): 896–905
- Lewis WM Jr (1981) Precipitation chemistry and nutrient loading by precipitation in a tropical watershed. *Water Resour Res* 17(1):169–181
- Li Z, Boyle F, Reynolds A (2010) Rainwater harvesting and greywater treatment systems for domestic application in Ireland. *Desalination* 260(1-3):1–8
- Lovett GM (1994) Atmospheric deposition of nutrients and pollutants in North America: an ecological perspective. *Ecol Appl* 4(4):629–650
- Lu X, Li LY, Li N, Yang G, Luo D, Chen J (2011) Chemical characteristics of spring rainwater of Xi'an city, NW China. *Atmos Environ* 45(28):5058–5063
- Marandi A, Polikarpus M, Joeleht A (2013) A new approach for describing the relationship between electrical conductivity and major anion concentration in natural waters. *Appl Geochem* 38:103–109
- Masood S, Saied S, Siddique A, Mohiuddin S, Hussain M, Khan M, Khwaja H (2019) Study of chemical composition in wet atmospheric precipitation in Karachi, Pakistan. In: *Recent advances in geo-environmental engineering, geomechanics and geotechnics, and geohazards*. Springer, Cham, pp 75–78
- Matawle JL, Pervez S, Dewangan S, Shrivastava A, Tiwari S, Pant P et al (2015) Characterization of PM_{2.5} source profiles for traffic and dust sources in Raipur, India. *Aerosol Air Qual Res* 15:2537–2548
- Meera V, Ahammed MM (2018) Factors affecting the quality of roof-harvested rainwater. In: *Urban Ecology, Water Quality and Climate Change*. Springer, Cham, pp 195–202
- Minerals and Geoscience Department Malaysia (2013) Geological map of Sarawak, third edition(1:750,000), Minerals and Geoscience Department Malaysia, Sarawak
- Moglia M, Walton A, Gardner J, Tjandraatmadja G (2015) Management and operational needs for urban rainwater tanks. *Rainwater Tank Systems for Urban Water Supply: Design, Yield, Energy, Health Risks, Economics and Social Perceptions*: 151-179
- Mouli PC, Mohan SV, Reddy SJ (2005) Rainwater chemistry at a regional representative urban site: influence of terrestrial sources on ionic composition. *Atmos Environ* 39(6):999–1008
- Nadzir MSM, Lin CY, Khan MF, Latif MT, Dominick D, Hamid HHA, Mohamad N, Maulud KNA, Wahab MIA, Kamaludin NF, Lazim MASM (2017) Characterization of rainwater chemical composition after a Southeast Asia haze event: insight of transboundary pollutant transport during the northeast monsoon. *Environ Sci Pollut Res* 24(18):15278–15290
- Neal C, Skeffington R, Neal M, Wyatt R, Wickham H, Hill L, Hewitt N (2004) Rainfall and runoff water quality of the Pang and Lambourn, tributaries of the River Thames, south-eastern England. *Hydrol Earth Syst Sci* 8(4):601–613
- Niu Y, Li X, Huang Z, Zhu C (2017) Chemical characteristics and possible causes of acid rain at a regional atmospheric background site in eastern China. *Air Qual Atmos Health* 10(8):971–980
- Nriagu JO (1990) Global metal pollution: poisoning the biosphere? *Environ Sci Policy Sustain Dev* 32(7):7–33
- Ojekunle ZO, Jinadu OOE, Afolabi TA, Taiwo AM (2018) Environmental pollution and related hazards at Agbara industrial area, Ogun State. *Sci Rep* 8(6482):1–8
- Oru  MR, Gaiero D, Kirschbaum A (2019) Seasonal characteristics of the chemical composition of rainwaters from Salta city, NW Argentina. *Environ Earth Sci* 78(1):16. <https://doi.org/10.1007/s12665-018-8007-0>
- Ouyang W, Xu Y, Cao J, Gao X, Gao B, Hao Z, Lin C (2019) Rainwater characteristics and interaction with atmospheric particle matter transportation analyzed by remote sensing around Beijing. *Sci Total Environ* 651:532–540
- Polkowska  , Astel A, Walna B, Ma ek S, M edrzycka K, G orecki T, Siepak J, Namie nik J (2005) Chemometric analysis of rainwater and throughfall at several sites in Poland. *Atmos Environ* 39(5): 837–855
- Postel SL (2000) Entering an era of water scarcity: the challenges ahead. *Ecol Appl* 10(4):941–948
- Radojevic M (2003) Chemistry of forest fires and regional haze with emphasis on Southeast Asia. *Pure Appl Geophys* 160(1-2):157–187
- Radojevic M, Lim LH (1995) A rain acidity study in Brunei Darussalam. *Water Air Soil Pollut* 85(4):2369–2374
- Radojevic M, Tan KS (2000) Impacts of biomass burning and regional haze on the pH of rainwater in Brunei Darussalam. *Atmos Environ* 34(17):2739–2744
- Rajeev P, Rajput P, Gupta T (2016) Chemical characteristics of aerosol and rain water during an El Ni o and PDO influenced Indian summer monsoon. *Atmos Environ* 145:192–200
- Rao PSP, Tiwari S, Matwale JL, Pervez S, Tunved P, Safai PD, Srivastava AK, Bisht DS, Singh S, Hopke PK (2016) Sources of chemical species in rainwater during monsoon and non-monsoonal periods over two mega cities in India and dominant source region of secondary aerosols. *Atmos Environ* 146:90–99
- Rao W, Han G, Tan H, Jin K, Wang S, Chen T (2017) Chemical and Sr isotopic characteristics of rainwater on the Alxa Desert Plateau, North China: implication for air quality and ion sources. *Atmos Res* 193:163–172
- Rogers P, Hall AW (2003) Effective water governance. *Global water partnership*, Stockholm
- Rosca C, Schoenberg R, Tomlinson EL, Kamber BS (2019) Combined zinc-lead isotope and trace-metal assessment of recent atmospheric

- pollution sources recorded in Irish peatlands. *Sci Total Environ* 658: 234–249
- Rusydi AF (2018) Correlation between conductivity and total dissolved solid in various type of water: a review. In: IOP conference series: earth and environmental science (Vol. 118, No. 1, p. 012019). IOP Publishing
- Sabuti AA, Mohamed CAR (2016) Distribution and source of trace elements in marine aerosol of Mersing, Johor, Malaysia. *J Oceanogr Mar Res* 4(146):2
- Sakihama H, Ishiki M, Tokuyama A (2008) Chemical characteristics of precipitation in Okinawa Island, Japan. *Atmos Environ* 42(10): 2320–2335
- Sanhueza E, Elbert W, Rondon A, Arias MC, Hermoso M (1989) Organic and inorganic acids in rain from a remote site of the Venezuelan savannah. *Tellus B Chem Phys Meteorol* 41(2):170–176
- Sapek B (2014) Calcium and magnesium in atmospheric precipitation, groundwater and the soil solution in long-term meadow experiments. *J Elem* 19(1):191–208. <https://doi.org/10.5601/jelem.2014.19.1.597>
- Shrestha S, Prasad Pandey V, Yoneyama Y, Shrestha S, Kazama F (2013) An evaluation of rainwater quality in Kathmandu Valley, Nepal. *Sustain Environ Res* 23(5):341–350.
- Singh K (2011) Chemical composition of atmospheric precipitation in different environments of Palampur (Doctoral dissertation, CSKHPKV, Palampur)
- Song F, Gao Y (2009) Chemical characteristics of precipitation at metropolitan Newark in the US East Coast. *Atmos Environ* 43(32):4903–4913
- Steinnes E, Lierhagen S (2018) Geographical distribution of trace elements in natural surface soils: Atmospheric influence from natural and anthropogenic sources. *Appl Geochem* 88:2–9
- Suescún D, León JD, Villegas JC, García-Leoz V, Correa-Londoño GA, Flórez CP (2019) ENSO and rainfall seasonality affect nutrient exchange in tropical mountain forests. *Ecohydrology*. <https://doi.org/10.1002/eco.2056>
- Sultan K (2012) Hydrochemistry and baseline values of major and trace elements in tropical surface waters of the Terengganu River (Malaysia). *Water Int* 37(1):1–15
- Szép R, Bodor Z, Miklóssy I, Niță IA, Oprea OA, Keresztesi Á (2019) Influence of peat fires on the rainwater chemistry in intra-mountain basins with specific atmospheric circulations (Eastern Carpathians, Romania). *Sci Total Environ* 647:275–289
- Tatsuta S, Shimada K, Chan CK, Kim YP, Lin NH, Takami A, Hatakeyama S (2017) Contributions of long-range transported and locally emitted nitrate in size-segregated aerosols in Japan at Kyushu and Okinawa. *Aerosol Air Qual Res* 17:3119–3127
- Topçu S, Incecik S, Atımtay AT (2002) Chemical composition of rainwater at EMEP station in Ankara, Turkey. *Atmos Res* 65(1-2):77–92
- Tsukuda S, Sugiyama M, Harita Y, Nishimura K (2006) Atmospheric phosphorus deposition in Ashiu, Central Japan—source apportionment for the estimation of true input to a terrestrial ecosystem. *Biogeochemistry* 77(1):117–138
- Tu X, Lu Y, Yao R, Zhu J (2019) Air quality in Ningbo and transport trajectory characteristics of primary pollutants in autumn and winter. *Atmosphere* 10:120. <https://doi.org/10.3390/atmos10030120>
- Uchiyama R, Okochi H, Ogata H, Katsumi N, Nakano T (2019) Characteristics of trace metal concentration and stable isotopic composition of hydrogen and oxygen in “urban-induced heavy rainfall” in downtown Tokyo, Japan; The implication of mineral/dust particles on the formation of summer heavy rainfall. *Atmos Res* 217:73–80
- Wang W, Primbs T, Tao S, Simonich SLM (2009) Atmospheric particulate matter pollution during the 2008 Beijing Olympics. *Environ Sci Technol* 43(14):5314–5320
- Xing J, Song J, Yuan H, Li X, Li N, Duan L, Qu B, Wang Q, Kang X (2017) Chemical characteristics, deposition fluxes and source apportionment of precipitation components in the Jiaozhou Bay, North China. *Atmos Res* 190:10–20
- Zeri M, Carvalho VSB, Cunha-Zeri G, Oliveira-Júnior JF LGB, Freitas ED (2016) Assessment of the variability of pollutants concentration over the metropolitan area of São Paulo, Brazil, using the wavelet transform. *Atmos Sci Lett* 17:87–95
- Zhang J, Liu CQ (2004) Major and rare earth elements in rainwaters from Japan and East China Sea: natural and anthropogenic sources. *Chem Geol* 209(3–4):315–326
- Zhang M, Wang S, Wu F, Yuan X, Zhang Y (2007) Chemical compositions of wet precipitation and anthropogenic influences at a developing urban site in southeastern China. *Atmos Res* 84(4):311–322
- Zhang Y, Sun S, Olsen SC, Dubey MK, He J (2011) CCSM3 simulated regional effects of anthropogenic aerosols for two contrasting scenarios: rising Asian emissions and global reduction of aerosols. *Int J Climatol* 31(1):95–114
- Zhang X, Jiang H, Zhang Q, Zhang X (2012) Chemical characteristics of rainwater in northeast China, a case study of Dalian. *Atmos Res* 116: 151–160
- Zhong ZC, Victor T, Balasubramanian R (2001) Measurement of major organic acids in rainwater in Southeast Asia during burning and non-burning periods. *Water Air Soil Pollut* 130(1-4):457–462

Publisher's note Springer Nature remains neutral with regard to jurisdictional claims in published maps and institutional affiliations.